Supplemental Digital Content

Materials and Methods S1

Briefly, the pancreas was enzymatically digested using purified Thermolysin and Collagenase blend (Vitacyte, Indianapolis, IN) and islets were purified from the digestion using continuous Optiprep gradient (density 1.11–1.06) and COBE 2991 blood cell processor (Gambro BCT, Inc., Lakewood, CO). Only fractions with >70% purity by Dithizone staining were combined for transplantation. Final islet preparations were enumerated by manual counting and sizing and converting islet particle number (IPN) to islet equivalents (IEQ) based on a 150-μm islet diameter. After isolation, islets were cultured in CMRL 1066 tissue culture media (Mediatech, Inc.; # 99-663-CV) until the encapsulation procedure. Hemipancreatectomy, islet isolation from the donor pancreatic tissue, encapsulation in CXCL12-containing alginate and implantation into the intraperitoneal cavity were all performed within a 6-hour window after the start of the initial surgery.

Materials and Methods S2

For the empty beads, a 200-μm nozzle was used with a flow rate of 10 ml/min, voltage at 1100 V, frequency of 1200 Hz, and an amplitude of 3. Settings for the first autologous islet microbeads were changed to a nozzle size of 300 μm, a flow rate of 15 ml/min, voltage of 1000 V, frequency of 1300 Hz, and an amplitude of 4. For

production of the second autologous islet microbeads, an air-flow system featuring an air-dripping nozzle of 400 μm diameter, was used instead. For this process, the settings were: air pressure 1013 mbar, alginate flow 1.7 ml/min and air flow 2.05 L/min. Following passage through the encapsulator, all beads were polymerized for 5 minutes in a beaker or a reaction vessel with 250 ml of 300 mOsmol $CaCl_2$ solution (Fluka, # 21114-1L) with a bar stirrer at a rate of 100%. All encapsulation procedures were performed in a laminar flow hood using sterile technique.

The volume of alginate used for each empty microbead run was 13.5 ml, which contained 13.5 μg of CXCL12. For the first islet-containing encapsulation run, the freshly digested NHP islets were spun down at 200 RCF for 2 minutes and the pellet was then resuspended in 5 ml alginate solution containing 5 μg CXCL12; for the second encapsulation run the NHP islets were filtered through a 70 μm cell strainer, spun down and the pellet resuspended in 3 ml alginate solution with 3 μg CXCL12.

All microbeads were allowed to cross-link in a sterile, endotoxin-free 300 mOsmol $CaCl_2$ solution for 5 min. After this, the microbeads were transferred to a 50 ml conical tube and the $CaCl_2$ solution was removed by washing either with ultrapure water (for empty microbeads) or tissue culture media (for autologous islets). 30 ml of normal saline was then added to the tubes containing empty microbeads with or without CXCL12 and 30 ml CMRL 1066 tissue culture media was added to the tubes containing the autologous islet microbeads. Tubes were transferred to the surgical site and Implantation occurred shortly afterwards. Characterization of the morphology (size and circularity) of microbeads was performed using image analysis software (ImageJ).

Assessment of microbead porosity was determined using a dextran assay. Formal

batch records were prepared for each microbead preparation that was transplanted into an NHP.

Materials and Methods S3

Briefly, the animal was taken to the surgical operating room where it was prepared for surgery and induced to surgical plain anesthesia with inhalational anesthetics. A 1.5-cm midline incision cranial to umbilicus was performed and a PE catheter was used to infuse the empty capsules into the abdominal cavity. The direction of the catheter tip was rotated to distribute the capsules evenly throughout the abdominal cavity. After final inspection and closure of abdominal wall the animals were returned to their cages and recovered from anesthesia under surveillance. Since these 1-month explants from first 2 animals were done without previous experience using microbeads in NHPs, we explored the impact of a washing solution to remove any surface contamination of the beads. We also looked at the effect of the lavage solution on the shape and size of the microbeads, as well as the effect of prolonged incubation time on the imaging of the microbeads.
In the context of autologous transplantation, a partial pancreatectomy was first performed and within 6 hours of initial surgery microbeads were implanted through the surgical opening. CBC, differential and clinical chemistry studies were performed pre- and postimplantation on all NHPs.
NHPs were evaluated at 1, 3, and 6 months after microbead implantation through surgical inspection of the peritoneal site. The evaluation procedure for each

animal at the 1- and 3-month time points involved surgical opening of the peritoneal cavity through a 5–10-cm midline abdominal incision from pelvis to the sternum. At final evaluation, a 20-cm length incision was performed to allow for full visual inspection of the abdominal cavity and retrieval of the majority of microbeads from the peritoneum. Peritoneal lavage was performed at each evaluation with 30–100 ml warm normal saline and peritoneal fluid and free microbeads were aspirated with a 60-ml feeding syringe. Up to 3 biopsies were taken from the peritoneal tissues using ligation and coagulation hemostasis. Aspirated microbeads were separated from the peritoneal lavage using a 100-μm cell strainer and stored on ice for later analysis. The remaining aspirate sample was stored at -80 ^{o}C. A sample of retrieved microbeads were examined using phase contrast microscopy. Additional samples were embedded in paraffin and 10-μm thick sections prepared for morphological analysis and hematoxylin and eosin staining.

Materials and Methods S4

Briefly, NHP blood was collected in a Na-citrate tube and kept on ice until PBMC isolation was performed. For the serum isolation 2.5 ml of fresh blood was transferred to a tube, and after the clot formation (~30 min at RT) it was spun down at 1000 x g for 10 min at 4 ^{o}C. Serum aliquots of 500 μl were stored at -20 ^{o}C/-80 ^{o}C in cryovials. To the remaining blood sample (~7.5 ml), a same volume of 1X PBS + 2mM EDTA (PBMC buffer) was added. Such diluted blood was layered over the 15 ml of 96% Ficoll-Pacque (1.077) and spun down at 400 x g for 30 min at 4 ^{o}C without breaks. The upper plasma

layer was aliquoted as 500 μl and stored at -20 °C/-80 °C. The layer of PBMCs was carefully transferred to the new 50-ml tube and fill up with PBMC buffer, mixed and spun at 300 x g for 10 min at 4 °C with brakes on. Supernatants were discarded and mononuclear cells in PBMC buffer were spun at 200 x g for 10 min at 4 °C with brakes on. This wash step was repeated one more time. The cell pellet was resuspended in an appropriate volume (2–3 ml) of cRPMI 1640 1X media (Mediatech, Inc., Ref# 15-040-CV) and the number of cells determined using a MoxiFLow reader according to manufacturer's recommendations (ORFLO Technologies, Cat # MXF001). Cells were diluted with freezing media (80% FBS and 20% DMSO) and the aliquots stored at -20 °C/-80 °C.

Plasma and intra-abdominal fluid aspirate samples were analyzed for the levels of 14 different cytokines using the ProcartaPlex™ Multiplex Immunoassay kit (eBioscience, Cat # EPX140-40040-901), and also for the level of CXCL12 using the Human CXCL12/SDF-1α Immunoassay kit (Quantikine ELISA kit, R&D Systems, Cat # DSA00), for all animals in this study, according to the manufacturer's protocols. The cytokine assay measures GM-CSF, IFNγ, IL-1β, IL-2, IL-4, IL-5, IL-6, IL-10, IL-12p70, IL-13, IL-17a, IL-18, IL-23, and TNF-α. Preliminary testing showed that a better cytokine signal was detectable in plasma as opposed to serum, so plasma was used as the source for the comparative testing. All samples of plasma and aspirate were run in duplicate on a 96 well. Standard curve for each cytokine was used to extrapolate the concentrations [Fluorescence Intensity (FI) - background data].

As the empty microbeads did not contain any islets, we only conducted a basic phenotypic characterization of circulating immune cell populations in the NHPs receiving empty microbeads. Analysis was done by multiparameter staining for CD3, CD4, CD8, CD20 and CD25. Briefly, a 96-well plate was loaded with cells ($1x10^6$/ml), spun at 1,500 rpm for 5 minutes and cells were resuspended with the combined CDs (APC-Cy7 Mouse Anti-Human CD3, PE Mouse Anti-Human CD4, V450 Mouse Anti-Human CD8, PerCP-Cy5.5 Mouse Anti-Human CD20, and BB515 Mouse Anti-Human CD25; BD Biosciences) and incubated for 30 min at 4 ^oC in dark. After 2 washes with FACS buffer, cells were fixed (1% PFA) for 30 minutes at 4 ^oC in dark. After 2 washes, cells were resuspended with FACS buffer and stored overnight at 4 ^oC. For the first autograft, flow cytometry was performed on PBMCs from before transplant through final assessment at the 6-month point. We evaluated the same basic phenotypic characterization of lymphocytes as for the empty microbeads by multiparameter staining for CD3, CD4, CD8, CD20, and CD25. For the 2nd autograft, procedure was different as a stimulation with PMA/Iono (PMA: phorbol 12-myristate 13-acetate at a concentration of 30–50 ng/ml; Iono: Ionomycin at 1 μg/ml) and staining with extracellular (CD3, CD4, and CD8) and intracellular (FITC Mouse Anti-Human CD107a, Alexa Fluor ® 700 Mouse Anti- Human IFNg, BV605 Mouse Anti-Human TNF; BD Biosciences and APC Anti-IL-10 human; Miltenyi Biotec) antibodies were performed. Also, the BD Cytofix/Cytoperm kit (BD Biosciences #554714) with a BD GolgiPlug (BD# 555029) were used.

Compensation controls were prepared using the Antibody Capture Bead Kit (VersaComp, Ref # B22804) and the Flow cytometry was performed using the BD Fortessa equipment in the MGH Core facility.

Results S5

We have used the Peprotech CXCL12 in previously-published murine studies. The identity and purity of the 2 proteins were evaluated by 21st Century Biochemicals in blinded fashion using mass spec and HPLC; we performed studies on endotoxin levels, protein aggregation and biological potency in our laboratory. The 2 proteins were identical with the published sequence for CXCL12α except for a missing initial amino acid at the N-terminus of the Almac-produced protein. The purity analysis showed that the Peprotech product had a higher purity level than the Almac product (92% vs. 85%). Based on these initial results, we selected the CXCL12 from Peprotech for further testing. Endotoxin contamination of this protein was minimal, with a concentration of ≤1 EU/mg. Aggregation testing showed that the CXCL12 was below detectable level of 1%. Finally, we evaluated biological activity using an established Jurkat cell migration assay, which showed a biphasic response curve with a significant (4.4-fold) increase in migration of Jurkat cells at 10 ng/ml. The CXCL12 from Peprotech therefore showed its amino acid sequence was identical to the natural protein and that it was highly pure, biologically active and did not aggregate in solution at intended use concentrations.

Results S6

We had previously used a 200-μm encapsulator nozzle for preparation of the empty microbeads and encapsulator settings were optimized to this nozzle size. However, many of these islets appeared to be larger than 200 μm in diameter (Figure S3A

–S3B) and, therefore, exceeded the nozzle size, creating the potential for this nozzle to fragment larger islets. We therefore switched to a 300 μm nozzle. Unfortunately, we did not have the opportunity to optimize the encapsulator settings for use with this nozzle as encapsulation had to be performed immediately after islet isolation. As a result, in this first run only about 6000–7000 microbeads were produced of a significantly larger and more variable size (1207 ± 164 μm) than the empty microbeads. The number of islets within these microbeads was also variable (Figure S3C). Circularity of the microbeads was measured at 0.96.

Samples of these islet containing microbeads were incubated in CMRL media for 1 and 24 hours to assess islet viability and function. Supernatants were removed and stored at -20 ^{o}C and later used to perform an insulin ELISA assay with 1:1000 and 1: 2000 dilutions of the samples in duplicate; sample media was used as a (-) control. Insulin concentration for the 1:1000 diluted samples at 1 hour was 39.0 ± 2.15 pM and for the 1:2000 diluted samples was 25.6 ± 4.6 pM. Insulin concentration for the 24 hour samples were 65.4 ± 16.76 pM and 47.9 ± 6.3 pM, respectively. We calculated the released insulin concentration per islets at a 1:1000 dilution based on 30 tested microbeads with an average of about 6 islets per microbeads.

The estimated number of isolated islets from the 2nd hemi-pancreatectomy was ~60 000 IEQ. This isolation showed a more significant variation in the size of the islets than the first one. Therefore, we removed the smaller islets by 70-μm filtration to obtain a more uniform range of islets for encapsulation (Figure S3G–S3H). This run yielded ~22 000 microbeads with a mean diameter of 670 ± 18 μm and a roundness of 0.975

(Figure S3I). The distribution of islets within these microbeads was also much better controlled than in the first autologous islet encapsulation run. Samples of these microbeads were assessed for islet viability and function using an insulin ELISA assay. These encapsulated islets appeared more functionally active than the first set: insulin concentration for the 1:1000 diluted samples at 1hr was 63 $\pm$ 0.03 pM and for the 24 hours samples was 285.01 $\pm$ 21.75 pM.

Results S7

While the number of observed embedded microbeads was highly limited and represented only a very small percentage of the 400 000 implanted microbeads, biopsy samples from the CXCL12 (-) implant appeared to show significant cellularization (Figure 2A–2B). In contrast, sections taken from the CXCL12 (+) microbeads appear to show markedly less cellularization, with many beads remaining cell free even while surrounded by a thin layer of mesenteric tissue (Figure 2E–2F). Histochemical analysis of recovered free microbeads from the 1-month assessment with H&E staining did not show any indication of cellularization or fibrosis on either the CXCL12 (-) or CXCL12 (+) microbeads (data not shown); no immunohistochemistry was performed due to the absence of any cellularization. Similarly, samples taken from the tissue debris left after the filtration of lavage showed that microbeads from both implants did not appear to be fibrosed or cellularized. Representative images are shown in Figure 2C and Figure 2G. Sections of the tissues used for H&E staining were also IHC stained using fibroblast and macrophage antibodies. Here, sections from the CXCL12 (-) implants showed more

fibrosis around the microbeads (Figure 2D) when compared to CXCL12 (+) samples (Figure 2H). In all sets of images, spaces that appear around the microbeads are artefacts of shrinkage during the tissue fixation process.

Histopathology at the 3-month evaluation demonstrated no cellular infiltration around the microbeads present in any of the biopsies (Figure 2I and Figure 2M). Blind biopsies were again taken at the 6-month time point. At this point, embedded microbeads now appeared for the most part to be surrounded by mesothelial cells as was seen in Figure 1O–1P; while the CXCL12 (-) microbeads showed fibrotic layers consistent with a foreign body reaction, the CXCL12 (+) tissues appeared normal as was demonstrated in Figure 1Q–1R. At this time, we also stained some of the microbeads recovered from the lavage. Neither the CXCL12 (-) or the CXCL12 (+) microbeads showed any cellularization (Figure 2J–2K, Figure 2N–2O).

At 6 month some physical damage appeared to have occurred during lavage or aspiration of the sample but there were no signs of cellularization or fibrosis, CXCL12 (-) shown in Figure 2L and CXCL12 (+) in Figure 2P.

Results S8

We evaluated changes in the frequency of specific immune cell populations in the 2 implant recipients through the first 3 weeks after implantation. A review of the changes in populations of $CD3^+CD4^+$, $CD4^+CD8^+$, and $CD20^+$ cells showed that these

populations were stable and that CXCL12 (+) microbead implant did not appear to affect the population distribution within PBMCs (data not shown). Representative example of a flow analysis is shown in Figure S4.

Results S9

Neither NHP had any significant recorded changes in behavior, appetite, or weight. In the first autograft recipient, there were no changes in CBC, differential, or serum chemistries over the course of the study. Despite clinical stability one of the NHPs was observed to have serum chemistry changes that were compatible with acute pancreatitis following partial pancreatectomy. In the second autograft recipient, WBC count and serum chemistry became abnormal in the first week. Levels of total protein and albumin fell below normal and alkaline phosphatase was slightly elevated. The overall WBC count was slightly elevated, specifically due to granuloma elevation. Finally, the hematocrit, hemoglobin, and red blood cell count were below normal. Serum chemistry abnormalities and WBC levels normalized by week 2; the anemia persisted out to 4 weeks but was resolved by the 3-month point. These metabolic and immune changes, as we discuss below, were likely due to the onset of pancreatitis secondary to the hemi-pancreatectomy.

Results S10

In the first autograft animal, the level of GM-CSF, IL-18, IL-5, and IL-6 showed

elevations of around 1.5–2x over baseline pretransplant levels (Figure 5A). In the second NHP, elevations in IL-18 and IL-6 were noted, with IL-6 levels increasing 4-fold at week 1, which was consistent with the changes in the WBC (Figure 5B). The elevation of cytokines in the second autograft NHP was more obvious in the peritoneal aspirate samples taken at one month and was likely due to the pancreatitis following partial pancreatectomy (Figure 5C).

In the 2 NHPs receiving autologous islet microbead implants, the plasma level of CXCL12 did not appear to change significantly compared to the pretransplant baseline levels of 690.15 $\pm$ 92.75 pg/ml and 456.16 pg/ml respectively (Figure 5D). The second autograft animal did show a trend to increasing in plasma CXCL12 levels from day 0 to day 90. This may have been related to wound healing responses as a result of post pancreatectomy pancreatitis. The IP aspirate samples decreased in the concentration of CXCL12 from week 4 through 6-month period (Figure 5E).

Results S11

For the first autograft recipient, there were no significant changes seen in immune cell populations over the course of the study (data not shown); a representative example of a flow analysis is shown in Figure S5. For the second autograft, the assessment was done on PBMCs from preimplant through week 4 (Figure S6). Because this NHP experienced a significant pancreatitis after surgery that affected the peritoneal cavity, we evaluated circulating immune cell populations further by stimulating the cells with PMA/Ionomycin and staining with extracellular (CD3, CD4, and CD8) and

intracellular antibodies (CD107a, IL-10, IFNγ, and TNF-α). There were no notable increases in positively-stained cell populations in response to PMA/Ionomycin treatment, except for a 119% increase in $CD3^+CD8^+$ cells at 7 days, and a significant increase in $CD3^+CD4^+IL\text{-}10^+$ cells at day 14 (283%) at day 14.

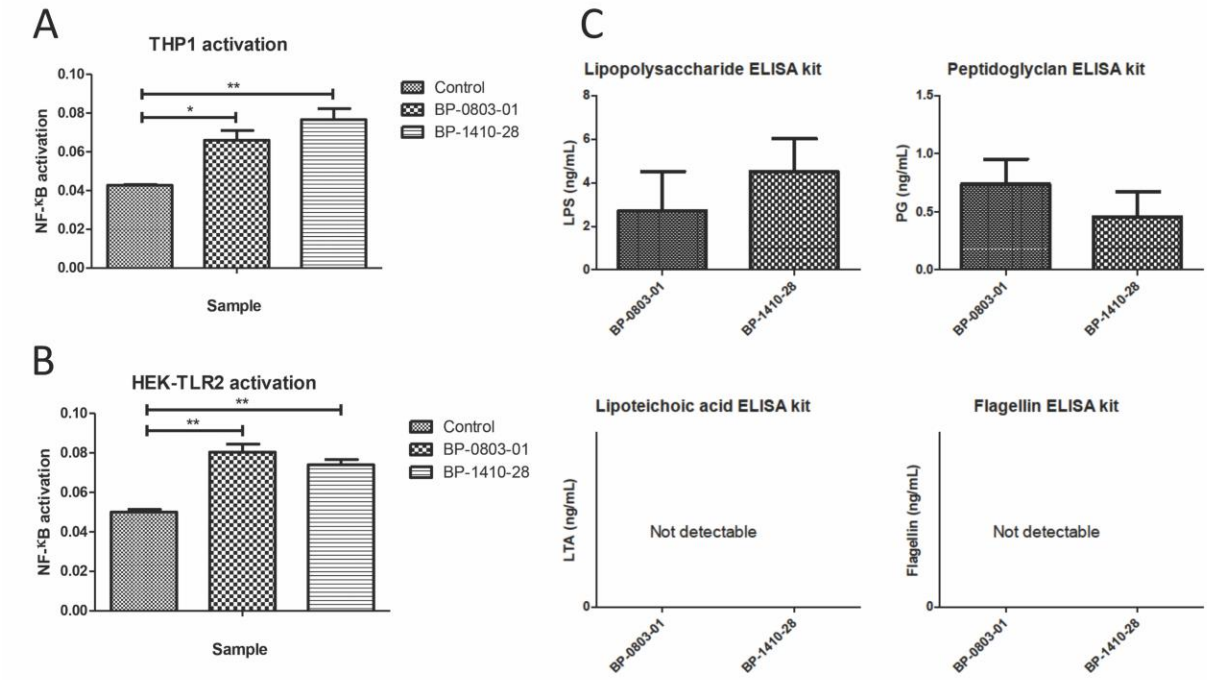

Figure S1. Testing the alginate immunogenicity. (A) THP1-XBlueTM-MD2-CD14 activation with the two alginate samples. (**B)** The HEK-Blue cell lines overexpressing TLR-2. (**C)** ELISA based analysis of the alginate samples for the presence or absence of PAMPs (lipopolysaccharide, peptidoglycan, lipotheichoic acid and flagellin).

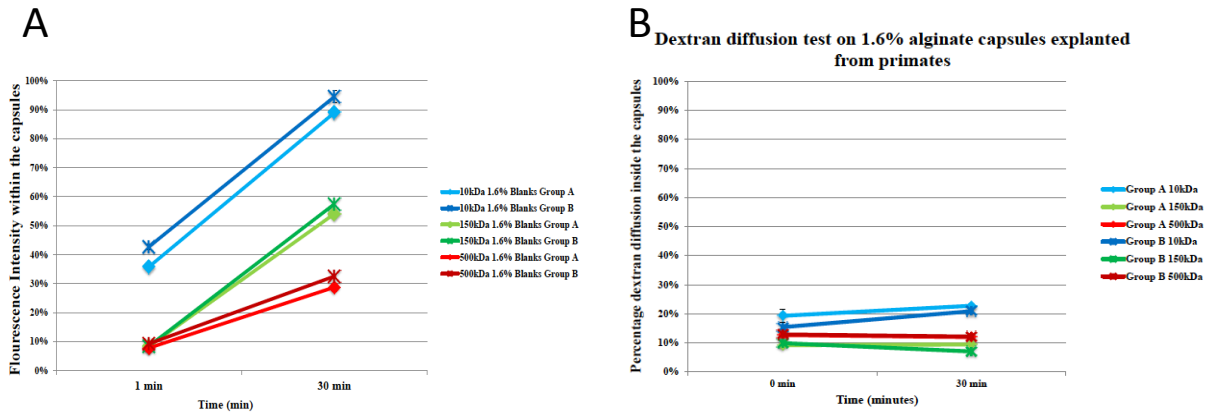

Figure S2. Preimplantation and 1-month postimplant microbead porosity studies. (A) Dextran diffusion analysis on empty microbeads preimplantation and (B) postexplant within 30 min.

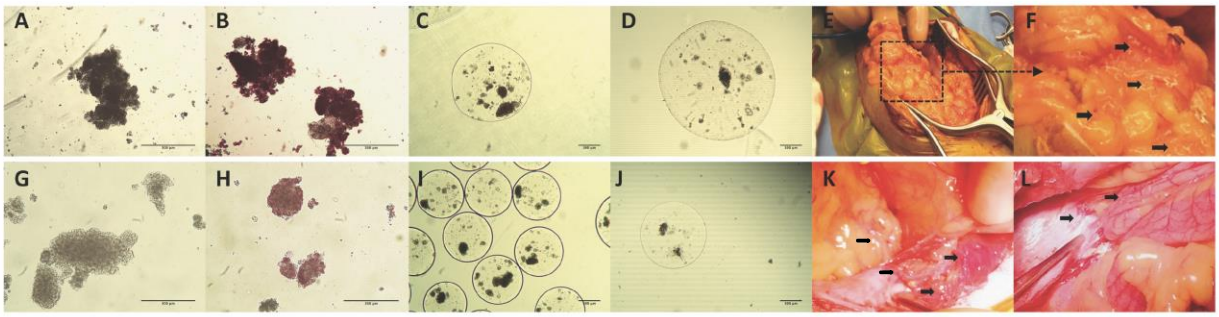

Figure S3. Images of the original autologous capsules pre-implant and appearance of the retrieved capsules at explant days. Top panel (**A - F**) showing the islets used for the 1st autograft. **(A)** Fresh unstained islets, (**B)** DTZ stained islets. **(C)** Images of microbeads pre-implantation, magnification 10x. **(D)** Image of the recovered free microbead at day 30 demonstrated the smooth and regular morphology with no sign of cellularization or fibrosis. The islets within the beads appeared intact and did not show obvious signs of necrosis, magnification 10x. **(E - F)** Biopsy at day 30 showing explanted tissues with visible microbeads (arrows). Bottom panel (**G - L**) showing the islets used for the 2nd autograft. **(G, H)** Images of the fresh and DTZ stained islets. **(I)** Uniform size and shape of the microbeads with islets distributed evenly within the capsules. (**J**) Retrieved free microbead at day 30, magnification 10x. **(K - L)** Biopsy at day 180 showing visible microbeads on the surface of the tissues.

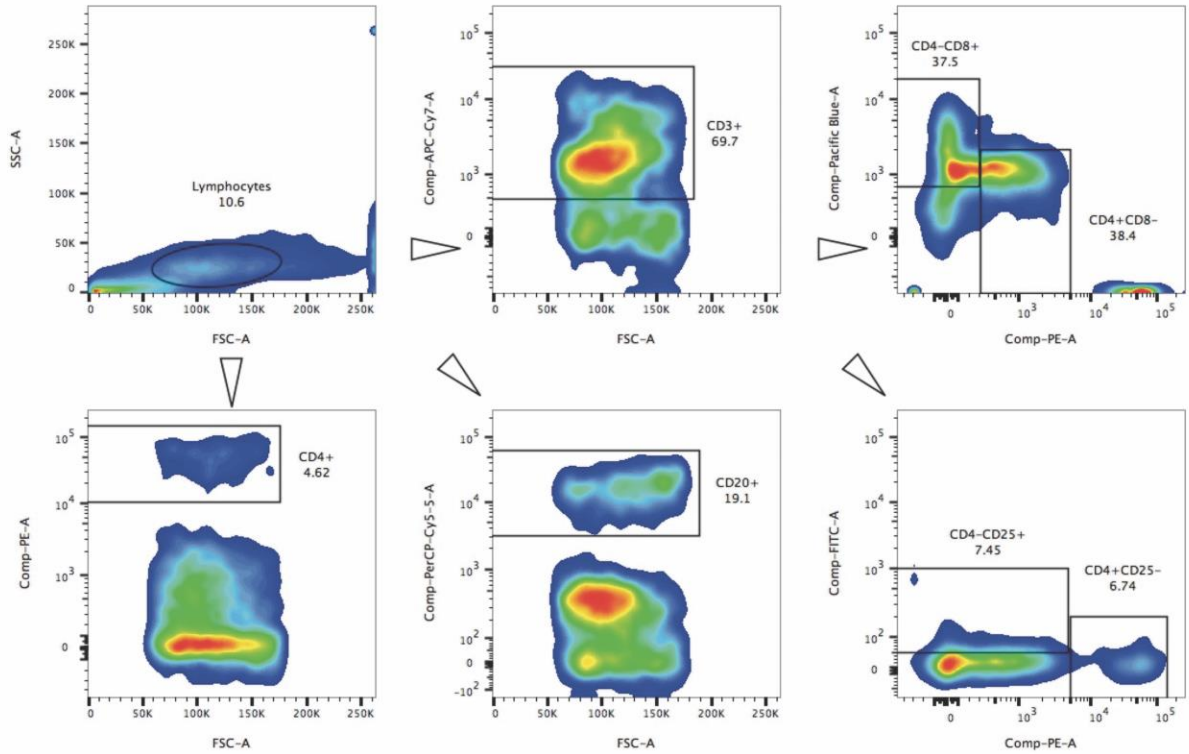

Figure S4. Gating strategy for identifying PBMC subpopulations in the empty NHPs study. A representative image from the flow cytometric analysis demonstrating gating strategy for identifying CD3+, CD4+, CD8+, CD20+ and CD25+ subpopulations.

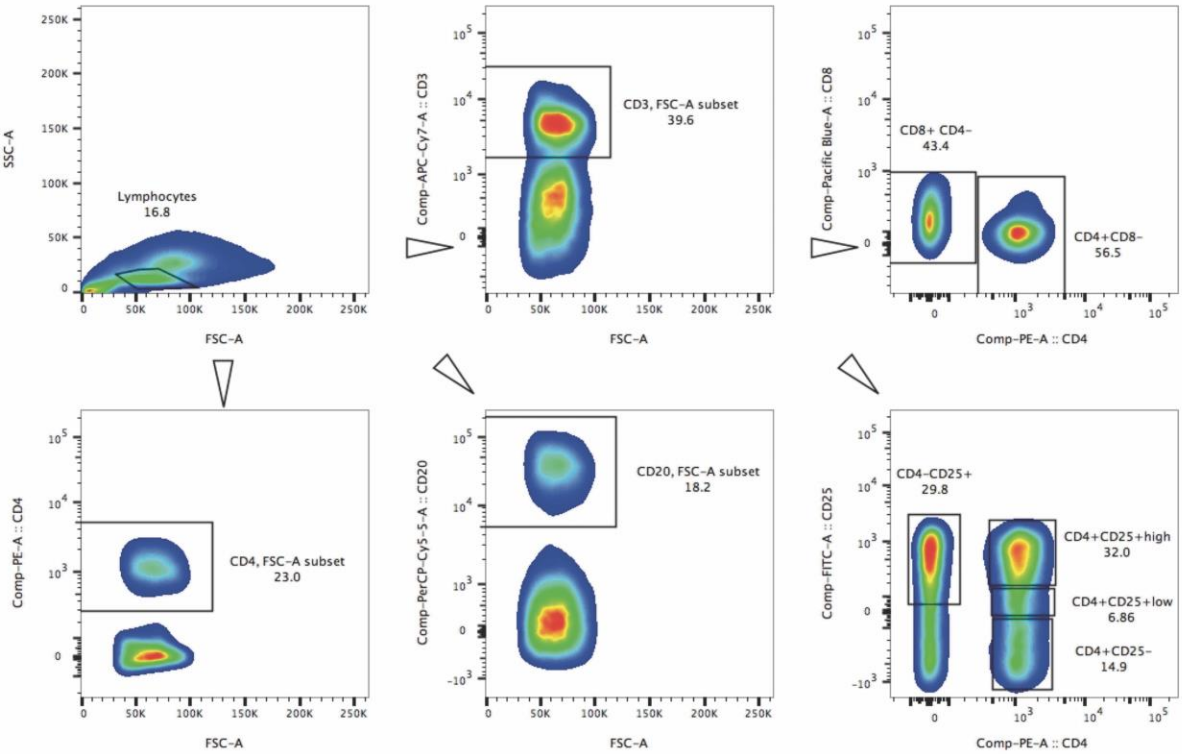

Figure S5. Gating strategy for identifying PBMC subpopulations in the 1st autograft study. A representative image from the flow cytometric analysis demonstrating gating strategy for identifying CD3+, CD4+, CD8+, CD20+ and CD25+ subpopulations.

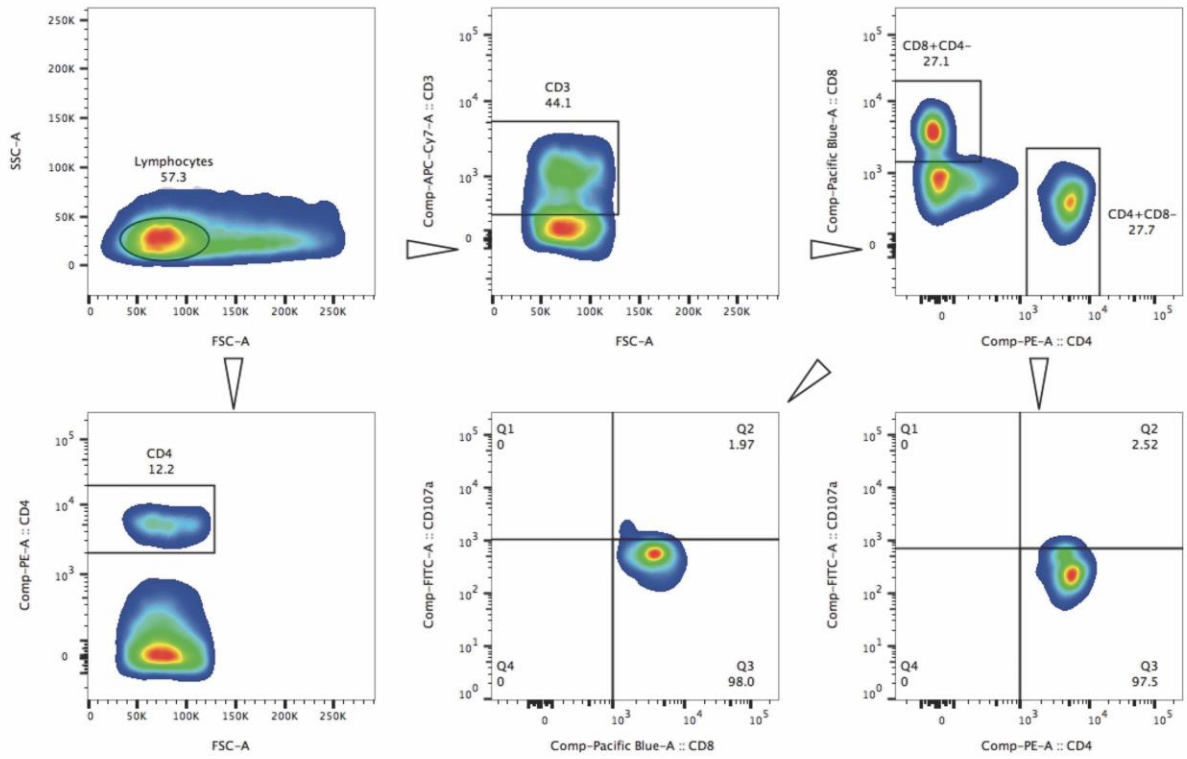

Figure S6. Gating strategy for identifying PBMC subpopulations in the 2nd autograft study. A representative image from the flow cytometric analysis demonstrating gating strategy for identifying CD3+, CD4+, CD8+ subpopulations and the specific cell markers (CD107a, IL-10, IFNγ and TNFα).